

# Transparent Antifouling Coatings Via Nanoencapsulation of a Biocide

M. Zhang, E. Cabane, J. Claverie

*Polymer Chemistry Research Group, Chemistry Department, University of Quebec at Montreal, Quebec, Montreal, Canada H3C3P8*

Received 29 March 2006; accepted 10 March 2007

DOI 10.1002/app.26659

Published online 11 June 2007 in Wiley InterScience (www.interscience.wiley.com).

**ABSTRACT:** Transparent coatings releasing an antifouling agent (AF) can be used to reduce the marine fouling of optical lenses. A variety of water-borne coatings based on poly(methyl methacrylate-co-butyl acrylate) (PMMA-co-PBA) were synthesized using a two-stage miniemulsion process. During this process, the AF, SeaNine 211, was nanoencapsulated in domains small enough not to scatter light. The release rate of SeaNine 211 was studied

for the polymers of different  $T_g$ , and found to be sufficient to impart AF properties. However, over time, the coatings were found to develop a whitish aspect (blushing) due to water retrodiffusion. © 2007 Wiley Periodicals, Inc. *J Appl Polym Sci* 105: 3824–3833, 2007

**Key words:** coatings; emulsion polymerization; nanoparticles; microencapsulation

## INTRODUCTION

Immersed optical instruments are widely used to monitor the marine environment and to inspect submarine installations. However, the efficiency of such instruments is dramatically limited in time by the fouling of the lens.<sup>1</sup> Over the years, a wide variety of approaches have been taken to provide antifouling (AF) properties to polymeric materials. Organotin compounds have been used for over 30 years, but they are now banned because of their detrimental environmental impact.<sup>2</sup> Foul-release coatings, most often silicon based, consist of coatings onto which organisms can settle but are removed by either mechanical or hydrodynamic cleaning.<sup>3</sup> Most silicon polymers are transparent and the use of a foul-release mechanism is an interesting strategy to prepare a transparent AF coating. However, immersed optical instruments often rest immobile, whereas a drag must be applied to remove settled organisms from this class of AF coatings. Biocidal AF coatings contain a biocide, which is released in the environment at a more or less controlled rate.<sup>4</sup> The biocide can be either directly compounded in the matrix (controlled depletion AF coatings) or

incorporated in a hydrophilic polymer via a hydrolyzable bond (self-polishing AF coating). To our knowledge, none of these coatings are transparent. In fact, many of them use copper oxide as biocide, which has a very strong visible absorption.

To be transparent, a polymeric coating must be devoid of chromophores in the visible region. It must also be index matched, which means that all the coating components (matrix and biocide) have the same refraction index. As an alternative to this last condition, the coating could be optically homogeneous, that is, to say homogeneous with a grain scale of roughly  $\lambda/10$ , where  $\lambda$  is the wavelength of light. In other words, the coating can be heterogeneous as long as the length scale of the heterogeneity is smaller than  $\lambda/10$ . Biocide-containing coatings are not transparent because the AF agent either is not transparent or is not homogeneously distributed in the coating. In this article, we show that nanoencapsulation, where the biocide is dispersed in domains typically smaller than 40 nm leads to transparent AF coatings.

To our knowledge, the preparation of transparent AF coatings has only been attempted a few times. Meinema et al. developed transparent organic-inorganic hybrid coatings with foul-release properties,<sup>5</sup> which were imparted by a thin film of polysiloxane (<10  $\mu\text{m}$ ) generated by the controlled hydrolysis of alkoxy methylsilanes  $R_n\text{Si}(\text{OR}')_{4-n}$ , where  $R = \text{Me}$ ,  $R' = \text{Et}$ ,  $n = 1$  or 2. Upon thermal curing, thin coatings that are Si—O—Si bonded to the glass substrate were formed. The organic methyl groups, pointing towards the surface, provided the hydrophobic character of the coating. The authors have also investi-

This work was performed at the University of New Hampshire.

Correspondence to: J. Claverie (claverie.jerome@uqam.ca).

Contract grant sponsors: The Coastal Ocean Observation and Analysis and the National Oceanographic and Atmospheric Administration.

*Journal of Applied Polymer Science*, Vol. 105, 3824–3833 (2007)  
© 2007 Wiley Periodicals, Inc.

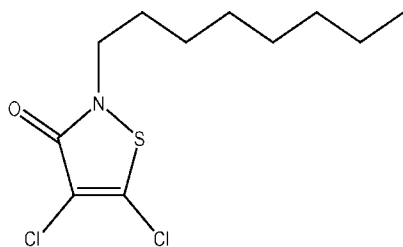


Figure 1 SeaNine 211.

gated the hydrophobic properties of the coatings with different methylsiloxane compositions and have correlated the surface activity to marine fouling. By increasing the hydrophobicity of the coating, biofouling can be drastically reduced. The methylsiloxane-based coatings containing fluorinated-alkylsilicon oxide moieties  $R_F\text{Si}(\text{OEt})_3$  ( $R_F = \text{CF}_3(\text{CF}_2)_5\text{CH}_2\text{CH}_2-$ ) are the most promising. The amount of biofouling, as measured by light microscopy numeration of the adsorbed species, can be reduced to some extent (20–40% compared to blank glass), but cannot be prevented completely.

Besides silicon-containing and fluorinated materials, other materials can be applied to produce the clear coatings. Parr et al. produced an hydrogel based on poly(2-hydroxyethyl methacrylate) (PHEMA) containing the biocide benzalkonium chloride (BAK). This hydrogel system is transparent and has the potential to be used on optical instruments in marine environment.<sup>6</sup>

In this work, we have decided to use 4,5-dichloro-2-octyl-3(2H)-isothiazolone (Seanine 211, Fig. 1) as biocide.<sup>7</sup> This compound allies excellent AF properties and acceptable environmental impact. It is also transparent in the window 300–900 nm (as measured by spectrophotometry). Our goal is to impart AF properties to a glass or quartz surface for a period of several months. In this first report, we concentrate on the description of the coating preparation, its properties, and the measurement of the release rates. In a further publication, we will describe the performance of the coating while tested in a marine environment.

## EXPERIMENTAL

### Materials and methods

SeaNine 211 (30 wt % in xylene) was kindly provided by the Rohm and Haas Company (Philadelphia, PA). Xylene was removed by rotary evaporation, yielding an off-white solid. NP-50, an uncharged polyethoxylated nonylphenol surfactant containing an average of 50 ethoxylate, was obtained from Rhône-Poulenc. Viscoatex 730, an ASE thick-

ener, was kindly supplied by Coatex (Genay, France). All other chemicals (methyl methacrylate (MMA), butyl acrylate (BA), ethylene glycol dimethacrylate (EGDMA), acrylic acid (AA), hexadecane, sodium dodecyl sulfate (SDS), potassium persulfate (KPS), potassium dichromate, sulfuric acid, and dimethyl dichlorosilane (DMDCS)) were purchased from Aldrich (Milwaukee) or Acros (Gent, Belgium) and were used without further purification, except for monomers, which were freshly distilled prior use.

Particle sizes were measured on a light scattering Microtrac VSR S3000 and on a capillary hydrodynamic chromatography CHDF 2000 from Matec Applied Instruments. Melting points and  $T_g$  were measured on a modulated DSC (Q100 TA Instruments). GC-MS analysis were run on a HP G1800C GCD gas chromatograph (Hewlett-Packard, Palo Alto, CA) interfaced to a HP mass-selective detector. Data acquisition and processing, and instrument control were performed by the HP MSD ChemStation software.

### Preparation of the polymers

The quantities used for each coating are listed in Table I. We give here a typical experimental procedure. The latexes were prepared in three steps: the monomers were first emulsified to form a stable miniemulsion, and then they were engaged in a miniemulsion polymerization to form a first-stage latex. In the last step, the first stage latex was grown using a semicontinuous addition of monomers. For each step, the polymerization reaction was followed by light scattering and gravimetry.

### Emulsification

A mixture of MMA, BA, and EGDMA (cross-linker), and SeaNine 211 was poured into an aqueous solution containing SDS and NP-50. This mixture was magnetically stirred for 20 min and sonicated with a Branson 450 ultrasonifier at 90% duty cycle and 90% output control at 0°C for 120 s.

### First stage

The miniemulsion was transferred into a 250-mL three-neck jacketed reactor equipped with a  $\text{N}_2$  inlet, a mechanical stirrer, and a reflux condenser. The initial charge was purged with nitrogen for 20 min and heated to 70°C. When this temperature was reached, a concentrated solution of initiator was injected with a syringe. The reactor was kept under nitrogen and heated for 2 h.

TABLE I  
Composition of Latexes Prepared by Two-Stage Miniemulsion Polymerization

| Experiment     |    | MMA<br>(g) | AF<br>(g) | EGDMA<br>(g) | SDS<br>(g)       | NP-50<br>(g) | KPS<br>(g) | Water<br>(g) | BA<br>(g) | AA<br>(g) |
|----------------|----|------------|-----------|--------------|------------------|--------------|------------|--------------|-----------|-----------|
| 1              | S1 | 22.4       | 7         | 0.92         | 0.6              | 0.4          | 0.03       | 102          |           |           |
|                | S2 | 25.0       |           |              | 0.7              | 0.4          | 0.03       | 15           | 25        | 1.47      |
| 2              | S1 | 22.4       | 7         | 0.92         | 0.6              | 0.4          | 0.03       | 102          |           |           |
|                | S2 | 23.8       |           |              | 0.6              | 0.4          | 0.03       | 10           | 23.8      | 1.47      |
| 3              | S1 | 5.5        | 3.7       | 0.52         | 0.3              | 0.2          | 0.02       | 50           | 7.6       |           |
|                | S2 | 12.1       |           |              | 0.3              | 0.2          | 0.02       | 6            | 12.0      | 0.69      |
| 4              | S1 | 7.0        | 3.5       | 0.50         | 0.4 <sup>a</sup> |              | 0.02       | 50           | 5.1       |           |
|                | S2 | 12.2       |           |              | 0.3 <sup>a</sup> |              | 0.02       |              | 13        | 0.70      |
| 5              | S1 | 4.8        | 3.5       | 0.42         | 0.3              | 0.2          | 0.02       | 51           | 6.38      |           |
|                | S2 | 11.9       |           |              | 0.3              | 0.2          | 0.02       |              | 11.9      | 0.94      |
| 6              | S1 | 8.3        | 4.4       | 0.52         | 0.3              | 0.2          | 0.02       | 51           | 4.7       |           |
|                | S2 | 12.5       |           |              | 0.3              | 0.2          | 0.02       | 5            | 12.5      | 0.7       |
| 7              | S1 | 8.5        | 3.6       | 0.54         | 0.2 <sup>a</sup> |              | 0.02       | 53           | 4.6       |           |
|                | S2 | 12.8       |           |              | 0.2 <sup>a</sup> |              | 0.02       | 5            | 12.7      | 0.7       |
| 8              | S1 | 11.8       | 5.25      | 0.69         | 0.4              | 0.3          | 0.3        | 76.5         | 5.0       |           |
|                | S2 | 17.9       |           |              | 0.4              | 0.3          | 0.3        | 10           | 17.8      | 1.1       |
| 9 <sup>b</sup> |    | 35.7       | 11        | 0            | 0                | 0            | 0.4        | 0            | 35.6      | 0         |
| 10             | S1 | 13.0       | 9.4       | 0.92         | 0.4              | 0.6          | 0.03       | 102          | 9.4       |           |
|                | S2 | 23.8       |           |              | 0.6              | 0.4          | 0.03       | 15.0         | 23.8      | 1.5       |

<sup>a</sup> For this experiment, PFOA (perfluorooctanoic acid) was used as surfactant.

<sup>b</sup> This is a solvent coating made by polymerizing MMA and BA first (using AIBN instead of KPS as initiator), then by incorporating the AF.

### Second stage

The second stage was started immediately after the completion of the first stage. The monomer mixture, MMA, BA and AA, and the aqueous solution, water, SDS, NP-50, and the initiator KPS were added continuously with a syringe pump. The addition rate was set in order to conduct the reaction under "monomer starved" conditions. After the addition was completed, the reaction mixture was reacted for an additional 30 min.

### Glass silanization

Chromerge, sulfuric acid, and DMDCS are corrosive, and all experiments were performed in a chemical fume hood using gloves, labcoat, and safety glasses. Chromerge is also excessively toxic, and should only be used with extreme caution. The chromerge solution was prepared by dissolving 20 g of potassium dichromate ( $K_2Cr_2O_7$ ) in 90 g of water, followed by the slow addition of 900 g of concentrated sulfuric acid. Glass substrates were washed with detergent, heavily rinsed with deionized water, and dried in an oven at 110°C. They were then rinsed with methanol and dried in an oven at 110°C and immersed in chromerge for a period of 30–60 s, carefully removed from the acid solution and rinsed three times with distilled water. The water-rinsed solutions were neutralized with sodium bicarbonate solutions before discarding. Finally, the glass substrate was rinsed with methanol

and blown dry using nitrogen. Using a 100-mL graduated cylinder, 50 mL of methylene chloride were mixed to 5 mL of dimethyldichlorosilane (DMDCS) and 45 mL of methylene chloride were added to reach the 100-mL mark. This solution was freshly made prior use, using thoroughly dried glassware. A glass substrate was totally immersed into the deactivation solution for 5–30 min (average 15 min). It was then rinsed with methylene chloride immediately after. Then, the substrate was covered with methanol for a period of 15–30 min, and the methanol was drained off and was blown dry using nitrogen.

### Film formation

The viscosity of latexes was increased using 1 wt % of the thickener Viscoatex 730 followed by addition of a few drops of concentrated ammonia. The film was then applied using an adjustable draw bar from Gardco (Universal Blade Applicator AP-G-02) and dried in air for 2 days. For solvent-borne films, the polymer was first dissolved in THF, applied with the draw bar, and dried in air. After the release experiment was completed, the film surface area was calculated from a digital picture of the film, and the film was detached from the glass substrate, dried, and weighed. From the weight and surface area, it was possible to assess an average film thickness, which corresponded well to the average thickness measured by light microscopy.

### Release tests

SeaNine 211 release tests were performed in artificial sea water, using the artificial sea water composition described in Ref. 8. The coated glass substrates were placed in beakers containing 1 L of seawater, which was changed daily. Each water volume was extracted with 100 mL of hexane. These samples were concentrated to 5 mL, and 0.5 mL of a decanol solution in hexane (100  $\mu\text{g}/\text{mL}$ ) was added. Decanol was used as an internal standard for GC/MS analysis. The concentration of the SeaNine 211 in hexane was determined quantitatively by using GC-MS. Analytes were separated on an Alltech AT<sup>TM</sup>-5MS (HP-5MS) capillary column (5% diphenyl/95% dimethylsiloxane), 30 m  $\times$  0.25 mm I.D., 0.50- $\mu\text{m}$  film thickness (plus 5 m guard). A split/splitless injector was used in the splitless mode. The injection-port liner was a deactivated single-tapered liner prepacked with glass wool. The injector operating conditions were optimized as follows: injection volume 5  $\mu\text{L}$ ; injector temperature: 250°C. The oven was programmed for 2 min at 40°C, followed by a ramp at 20°C/min up to 270°C (held 5 min) and the transfer line temperature was set at 280°C.

## RESULTS AND DISCUSSION

### Solvent-based coatings containing SeaNine 211

Arguably, the easiest method to make an AF coating consists in dissolving SeaNine 211 and a polymer in a common solvent, applying the viscous solution on a substrate and letting it dry. If the polymer, like SeaNine 211, is devoid of chromophores and if the AF agent is soluble in the polymer, a transparent coating should be obtained. Xylene and tetrahydrofuran (THF) were used as solvents and polymethyl methacrylate (PMMA), polybutyl acrylate (PBA), polyvinyl acetate (PVA), and polydimethyl siloxane (PDMS) were chosen as polymeric matrices. Using PDMS or PMMA, and THF or xylene as solvents, a white coating is obtained. Visual observation by light microscopy (Fig. 2) indicates that SeaNine 211 has phase separated from the film into macroscopic domains that scatter light. SeaNine 211 was found to be compatible in PBA and in PVA, but these two polymers are too tacky for our application.

To further confirm the phase-segregation phenomenon, the coatings have been characterized by DSC. If phase separation occurs, both the melting point of SeaNine 211 ( $T_m = 43^\circ\text{C}$ , as measured by DSC, Table II, line 1) and the  $T_g$  of the polymer should be observed. If SeaNine 211 is dissolved in the polymer, it should act as a plasticizer for the polymer, resulting in the lowering of the polymer  $T_g$ , and the absence of  $T_m$  for SeaNine 211. Fragments of the sol-

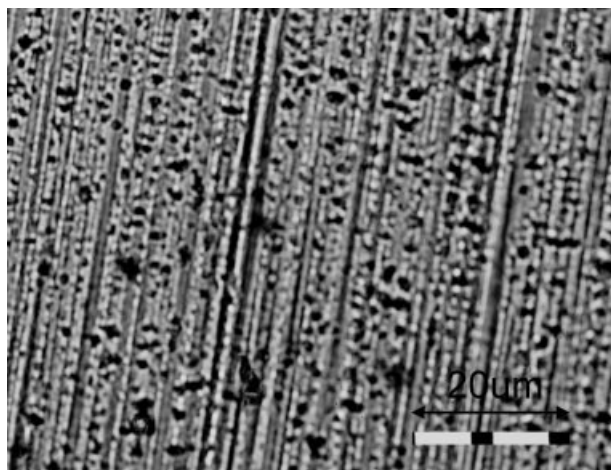


**Figure 2** Optical microscopy cliché of a solvent cast PMMA film containing 10 wt % of SeaNine 211. The black spots correspond to SeaNine 211 domains. The striations are generated by the bottom substrate (aluminum foil).

vent cast PMMA-based coatings were analyzed by DSC (Table II). In all cases, the melting of SeaNine 211 was observed, indicative of phase separation. However, a lowering of the polymer  $T_g$  was also observed, indicating that part of the SeaNine 211 is plasticizing the polymer. The latent heat of fusion was found to be  $\Delta H_f = 116 \text{ J/g}$  for a pure SeaNine 211 sample. Knowing the amount Wt(AF) of SeaNine 211 present in the coating analyzed by DSC, it is possible to calculate the percentage  $x$  of SeaNine 211, which is phase separated:

$$x = 100 \frac{\Delta H_{\text{SeaNine}}}{\text{Wt}(\text{AF})\Delta H_f} \quad (1)$$

where  $\Delta H_{\text{SeaNine}}$  is the area under the melting transition of SeaNine 211.

As seen in Table II, only small portions of the AF have phase separated (Wt(AF) dissolved – Wt(AF)), but it is always enough to prevent the coating from being transparent. Further examination of Table II indicates that for experiments 2–4, the amount of solubilized AF (in wt %) increases when  $T_g$  decreases. A plot of  $1/T_g$  vs  $w_{\text{AF}}$  is linear ( $r^2 = 0.98$ ), with a slope of  $3.50 \times 10^{-3}$  and an intercept of  $2.47 \times 10^{-3}$ . It is well known that the  $T_g$  of a mixture plasticizer polymer can be related to the individual properties of the plasticizer and polymer and their relative weight fractions, as long as the amount of plasticizer is limited.<sup>9</sup> For experiments 2–4, a Fox law<sup>9</sup> is followed, as shown by an inverse linear relationship between  $T_g$  and wt(%) of dissolved AF, yielding the expected values of 131°C for the  $T_g$  of PMMA and  $-105^\circ\text{C}$  for the  $T_g$  of the AF. Coatings having higher percentage of dissolved AF (such as experiment 6) do not follow anymore a Fox law, in

TABLE II  
Melting Point of SeaNine 211 in Solvent-Based PMMA Coatings: Analysis by DSC

| AF (wt %) | Coating (mg) | Wt (AF) (mg) | SeaNine 211 ( $T_m$ , °C) | $x$ (%) | Weight of dissolved AF (mg) | Dissolved AF (wt %) | First pass ( $T_g$ , °C) |
|-----------|--------------|--------------|---------------------------|---------|-----------------------------|---------------------|--------------------------|
| 100       | NA           | 6.2          | 43                        | 100     |                             |                     |                          |
| 3         | 15           | 0.44         | 51.4                      | 50      | 0.22                        | 1.5                 | 124                      |
| 6         | 23           | 1.36         | 52.4                      | 8       | 1.25                        | 5.4                 | 102                      |
| 9         | 23           | 2.04         | 52.6                      | 22      | 1.59                        | 7.0                 | 99                       |
| 12        | 33           | 3.96         | 50.6                      | 4       | 3.80                        | 11.5                | NO                       |
| 15        | 20           | 3.00         | 49.0                      | 10      | 2.70                        | 13.5                | 128                      |
| 18        | 17           | 3.06         | 53.0                      | 5       | 2.91                        | 17.1                | NO                       |

The weights correspond to the weights of the DSC sample. NO, not observed.

agreement with other reports concerning the  $T_g$  of highly plasticized matrices.<sup>9</sup>

Interestingly, the melting point of SeaNine 211 in PMMA was found to be significantly higher than the one measured for pure SeaNine 211. We first believed this difference could be attributed to a chemical modification of SeaNine 211 in the coating. We have separated SeaNine 211 from the PMMA matrix (using an extensive hexane wash) and found, using GC-MS, that the leached compound is unmodified SeaNine 211. Alternatively, we believe SeaNine 211 melting may be delayed because it is confined in a solid matrix, preventing its volume expansion upon melting. When the temperature increases in the DSC past the standard melting point of SeaNine 211 (standard = 43 °C, stage 1 in Fig. 3), a steep increase in pressure occurs in the SeaNine 211 domains, since those domains cannot melt (stage 2, Fig. 3). Eventually, the pressure is so elevated that the PMMA matrix collapses to release the pressure

(stage 3). The pressure nearly instantaneously decreases and SeaNine 211 melts immediately (stage 4). The pressure at which the matrix collapses can be evaluated from the Clausius–Clapeyron equation:

$$\frac{dP}{dT} = \frac{\Delta H}{T \Delta V} = - \frac{\Delta H_f \Delta \rho}{T \rho^2} \quad (2)$$

where  $P$ ,  $\rho$ , and  $T$  are the pressure, liquid density, and temperature at which the melting occurs,  $\Delta H$  is the heat exchanged during the melting,  $\Delta H_f$  is the heat of fusion (heat exchanged per unit mass), and  $\Delta \rho$  is the density difference between solid and liquid. Using the value  $\Delta H_f = 116$  J/g (Table II), and very approximate densities of  $\rho = 1.1$  g/cm<sup>3</sup> and  $\Delta \rho = -0.1$  g/cm<sup>3</sup>, the pressure increase is of 44 atm/K = 660 psi/K. An elevation of 10 K corresponds to a pressure increase of 6600 psi, which is close to the tensile strength of PMMA (reported to be between 8250 and 12000 psi).<sup>10</sup> Thus, the increase of SeaNine 211 melting point may be explained by its confinement in an incompressible matrix.

To summarize this section on the compatibility of SeaNine 211 in a solvent-based acrylic coating, it appears that the AF is nearly totally solubilized in the polymer, indicating that SeaNine 211 is virtually miscible. However, during the film formation, a small fraction of the SeaNine 211 crystallizes, thus generating a non transparent film. This phenomenon is frequently observed in solvent-borne coatings,<sup>11</sup> where the solvent evaporates rapidly. At the air/coating interface, the solvent is depleted, resulting in large concentration heterogeneity and eventually phase separation. Thus, the phase separation of SeaNine 211 from the film is a kinetically driven process. To further prove that SeaNine 211 is soluble in PMMA, a film of PMMA containing 10% of AF was heated for 12 h at 150 °C (above the  $T_g$  of PMMA). The film was then cooled over a period of 6 h to 50 °C, and brought quickly to room temperature. The film was found to be transparent, but a slight yellow tinge had developed, making it unusable for optical observations.

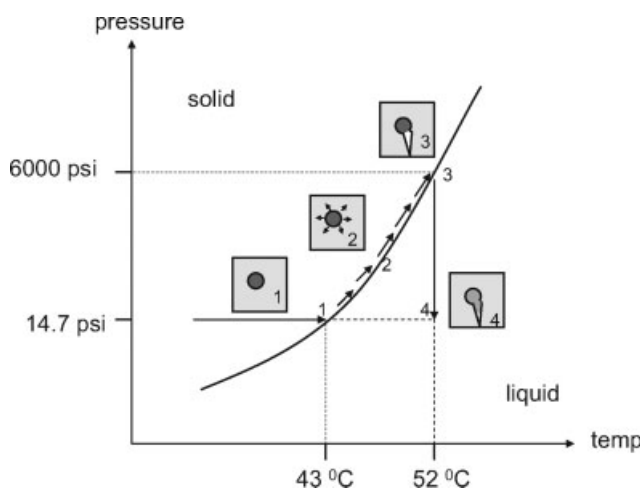


**Figure 3** Phase diagram illustrating the melting of solid SeaNine 211 in a PMMA matrix. In (1), the AF is reaching its melting point at  $P = 1$  atm, resulting in a volume expansion as the temperature increase (2), followed by a rupture of the polymeric matrix (3), and an immediate melting (4).

**TABLE III**  
Average Particle Size of a Latex Prepared by Miniemulsion Polymerization of MMA (20 wt% in Water), Stabilized by 5 g/L of SDS

| Hydrophobe<br>(wt %) <sup>a</sup> | Hexadecane                | SeaNine 211               |
|-----------------------------------|---------------------------|---------------------------|
|                                   | Particle<br>diameter (nm) | Particle<br>diameter (nm) |
| 2                                 | 62.2                      | 60.8                      |
| 5                                 | 86.9                      | 89.7                      |

<sup>a</sup> Relative to the monomer.

### Nanoencapsulation of SeaNine 211 by miniemulsion polymerization

Since solvent-based coatings are not transparent, a strategy has been devised to prepare aqueous-based coatings. Miniemulsion polymerization is now a well-established technique whereby a metastable o/w emulsion of a monomer is prepared, which is later radically polymerized.<sup>12</sup> The emulsion is stabilized by the right choice of surfactant and Ostwald ripening is prevented by the addition of a small amount of a hydrophobe, which does not have the capacity to diffuse through the aqueous phase. Most often, hexadecane or an oligomer of polystyrene is used as hydrophobe, but it has been shown that numerous other compounds can be used.<sup>13</sup> In our case, SeaNine 211 was chosen as hydrophobe, because its aqueous solubility is low. Usually, up to 5 wt % relative to the monomer phase is used as hydrophobe in a miniemulsion polymerization. If we assume that monomer droplets of 100 nm are prepared, then the maximum size of the domain occupied by SeaNine 211 fully phase separated is  $\sim (0.05)^{1/3} 100 \text{ nm} = 36 \text{ nm}$ , which is small enough not to scatter light (see above). This characteristic size is calculated assuming that all the AF is phase separated into one single domain in a latex particle. In fact, it is conceivable that the AF is not phase separated, or phase separated in a series of smaller domains.

As shown in Table III, SeaNine 211 is as efficient as hexadecane to stabilize a miniemulsion of MMA. In all cases, the resulting latexes were obtained without any coagulum. Interestingly, SeaNine 211 solubility in water (6 ppm)<sup>14</sup> is far greater than the one of hexadecane<sup>15</sup> (<1 ppb) and compares to the solubility of heptane (2 ppm), which cannot be used to prevent Ostwald ripening. The propensity of SeaNine 211 to stabilize the emulsion may be attributed to an amphiphilic character of SeaNine 211 (polar head formed by the thiooxazoline, and hydrophobic alkyl tail). Besides, visual observations of the miniemulsion indicated that large amount of foam was generated during the emulsification of MMA in the presence of SeaNine 211.

Since SeaNine 211 can be used to stabilize a miniemulsion, a family of acrylic latexes was prepared by

a two-stage process. The first stage is consisted in the preparation of an acrylic latex at 20% solid content by miniemulsion polymerization, using 20 wt % SeaNine 211 as "hydrophobe." These latex particles are crosslinked because the acrylic monomers contain 2–5 wt % of EGDMA. In the second stage, another batch of acrylic monomers and additional surfactant is added continuously to the latex to reach a final solid content of 40 wt%. The second stage occurs under so-called starved conditions: the instantaneous conversion, as measured by gravimetry, is always above 80%. The number of particles before and after the second stage is identical, indicating the absence of renucleation.

As this system is an entirely aliphatic acrylic system, the evaluation of the morphology of the particles proved to be difficult, due to the absence of selective staining agents.<sup>16–18</sup> We loosely name these particles as "core-shell" structures, but we are aware that in fact these particles may not be core-shell at all. On the basis of the work by Sundberg et al. on latex particle morphology,<sup>19,20</sup> we can assume that the second stage polymer is not occluded in the first stage because the first stage is crosslinked, and the second stage polymer phase is in contact with the aqueous phase. The external layer of the particle must have a low  $T_g$  for the latex to be able to form a film upon drying at ambient temperature. In our case, the second stage polymer is on the external layer, and its  $T_g$  is always low enough to allow for film formation (see Table IV). Upon drying, this soft layer will deform to occupy the void between the close-packed core particles.

All our latexes are copolymers of poly(methyl methacrylate-*co*-butyl acrylate) (PMMA-*co*-PBA). PBA has a refractive index of 1.4830 and atactic PMMA of 1.4899.<sup>21</sup> Since these two values are very close, blends of copolymers of PBA-*co*-PMMA, PBA, and PMMA, even when phase separated, are often transparent (index matching).

**TABLE IV**  
Characteristics of the Films Used in the AF Release Experiments

| Experiment     | $T_g$ of the<br>core (°C) | $T_g$ of the<br>shell (°C) | AF released<br>after 1<br>month (%) | Thickness<br>( $\mu\text{m}$ ) |
|----------------|---------------------------|----------------------------|-------------------------------------|--------------------------------|
| 1              | 115                       | 115                        | <0.1                                | 112                            |
| 2              | 115                       | 15.6                       | <1.0                                | 85                             |
| 3              | 6.6                       | 14.3                       | 2.46                                | 210                            |
| 4              | 28.1                      | 13.2                       | 2.54                                | 113                            |
| 5              | 32.0                      | 20.0                       | 18.1                                | 57                             |
| 6              | 38.4                      | 15.4                       | 1.91                                | 114                            |
| 7              | 40.7                      | 15.9                       | 2.77                                | 159                            |
| 8              | 49.9                      | 15.6                       | 2.98                                | 110                            |
| 9 <sup>1</sup> | NA                        | 15.6                       | 5.06                                | 127                            |

<sup>a</sup> This film is a solvent borne film.

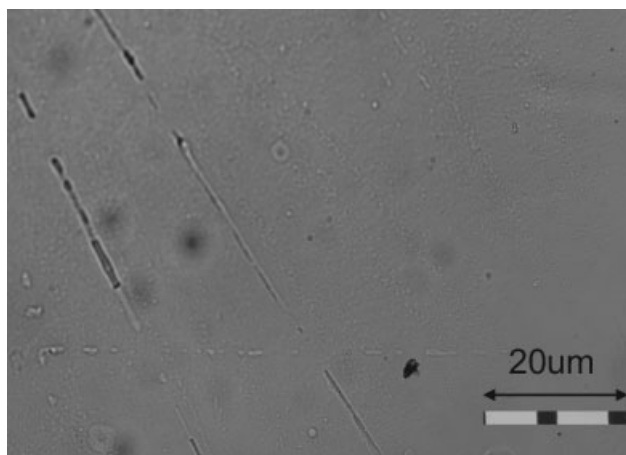


**Figure 4** Optical microscopy cliché of the latex-based coating on a glass slide (50 $\times$  magnification).

#### Coating formation using the two-stage latex

Latexes were applied on a glass slide using a slide bar, and left to dry in ambient air for 3 days. The resulting film was transparent (Fig. 4), but quickly delaminated from the glass substrate upon immersion in water. Glass surface being essentially hydrophilic, large capillary forces develop in water, resulting in complete loss of adhesion. Glass was then silanized with dimethyl dichlorosilane, thus blocking most of the surface silanol groups. When the hydrophobic glass substrate was coated with the latex, the resulting film adhered to the substrate, even after immersion in water for 3 months. Such films are transparent and homogeneous (no phase separated domains). As shown in Figure 5, the DSC trace of the film containing 10 wt % of SeaNine 211 indicates

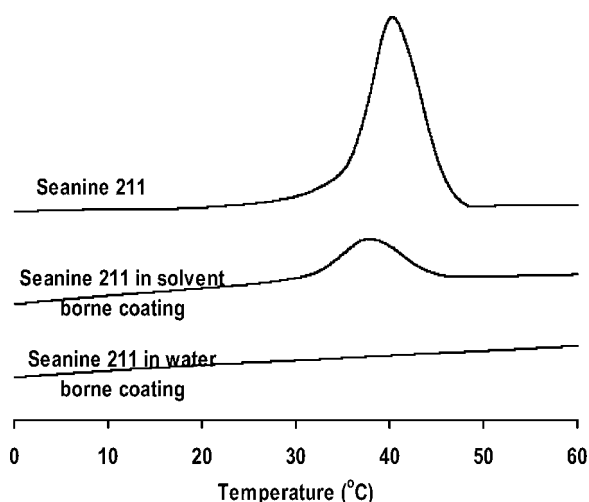


**Figure 5** DSC traces of the coating containing SeaNine 211 and the acrylic polymer. For the sake of clarity, the traces have been scaled and translated in the  $y$  direction. Solvent coating: coating 8, aqueous borne coating: coating 4.

that the polymer is plasticized by SeaNine 211 and no melting point of SeaNine 211 is observed, indicating the absence of large Seanine crystals.

With time, the coatings blushed, indicating the presence of heterogeneities in the coating. Blushing is a common behavior in water borne coatings and it is usually ascribed to the selective absorption of water in the surfactant-rich domains that may preserve the memory of the former particles (and thus result in visible light scattering) if particle coalescence is not complete. Blushed coatings were detached from the glass slide using a razor blade, and were analyzed by DSC. The resulting traces are virtually identical to those of the initially transparent coating, indicating that the blushing is not due to phase separation of SeaNine 211. Upon drying, the coating became transparent, and when subsequently immersed in water, the coating blushed again. Therefore, we attribute the blushing phenomenon to uptake of water by the coating. Water uptake by acrylic resins can be quite significant (Fig. 6) and rapid. The water uptake is measured by the relative weight increase of a film immersed in water. Rigorously, it would be necessary to subtract the weight of released SeaNine 211 to the weight gain. However, it will be seen below that SeaNine 211 released in the time scale of the uptake experiments is significantly less than the weight gain due to water uptake.

The water-uptake experiments were conducted on 100- $\mu$ m thick films, which were detached from the glass slide. In Figure 6, the composition of the core of the particles has been changed, but the composition shell is 50% butyl acrylate 50% methyl methacrylate in all cases. Overall, the composition of the three coatings are quite similar (34, 38, and 40% in

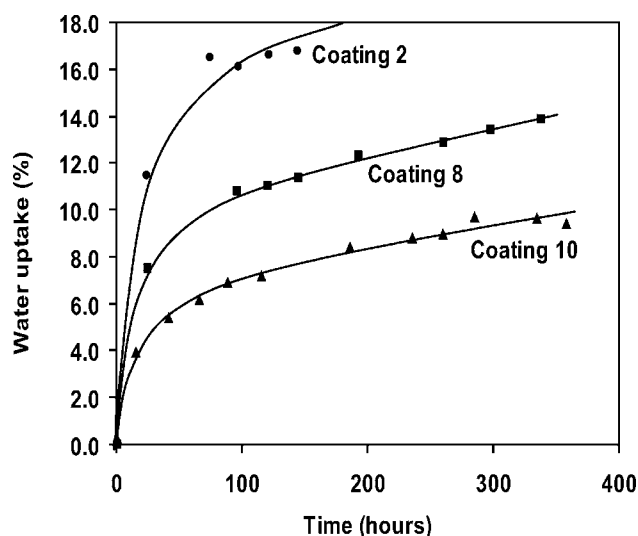


**Figure 6** Water uptake of several films. The composition of each coating can be found in Table I. The lines are here to guide the eyes only.

butyl acrylate, respectively), yet there are significant differences in water uptake. For the sake of completion, it is important to state that water uptakes were found to significantly depend on the nature and amount of surfactant and inorganic salt used during preparation of the latex, a phenomenon, which is already amply described in the literature.<sup>22</sup> Solvent-based coatings were found to have low water uptake, as expected in the absence of surfactants and salts.

### Release of SeaNine 211 from the coating

Coated glass samples were immersed in artificial seawater at 25°C.<sup>23</sup> The water was changed at regular intervals, and analyzed to assess the AF concentration, which was always below its solubility limit thus ensuring that there always existed a driving force for the SeaNine 211 to diffuse out.

A minimum flux of 10  $\mu\text{g}/\text{cm}^2/\text{day}$  is necessary to ensure AF properties.<sup>24,25</sup> Our final goal is to release SeaNine 211 at a flux higher than this threshold value for the largest possible number of days. For a coating, having a 100- $\mu\text{m}$  thickness containing 10% SeaNine 211 (average thickness and loading of our coatings), a 1  $\text{cm}^2$  section contains 10 mg of SeaNine 211. For an ideal zero-order release profile occurring at the threshold rate, SeaNine 211 would be released in 1000 days (3 years). Therefore, a coating loaded with 10% SeaNine 211 would contain enough AF to be efficient over a few months (our target duration). As seen below, the coating is never fully depleted of AF.

Figure 7 represents the cumulative amounts of released AF (% released) versus time for several coatings. The cumulative amount is directly proportional to the cumulative flux ( $\mu\text{g}/\text{cm}^2$ ) for coatings with given thickness and initial load of AF. All coatings have the same AF loading (10% wt:wt), and an average thickness of 118  $\mu\text{m}$ , except for one sample. The cumulative flux is the integral value of the instantaneous flux ( $\mu\text{g}/\text{cm}^2/\text{day}$ ), which is the quantity accessed experimentally. The measured instantaneous flux is a very noisy quantity, and, for the sake of practicality, we have averaged out the noise by looking at the cumulative flux. For the top curve, the release rate is high enough to impart AF properties. The two next ones would be marginally acceptable (flux of 3–15  $\mu\text{g}/\text{cm}^2/\text{day}$ ), but the coating of the bottom curve is not expected to be antifouling.

Several factors are believed to influence the release rate, such as coating thickness, core and shell composition. In Figure 7 and Table IV, comparing coating 5 to coating 4, it is clear that, for similar compositions, thickness strongly influences the release rate, as measured in % AF release. Obviously, a thin coating would be depleted faster, and the % AF released would be significantly greater. Therefore, to compare

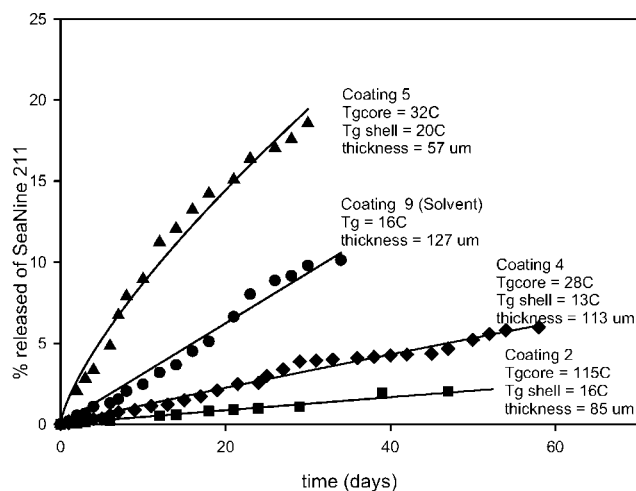


**Figure 7** Cumulative amount of released AF (relative to total amount encapsulated) versus time. The lines correspond to curve fits with  $y = ax^b$ . Triangles: Coating 5 ( $b = 0.73$ ), circles: Coating 9 ( $b = 1$ ), diamonds: Coating 4 ( $b = 0.94$ ), Squares: Coating 2 ( $b = 0.96$ ).

release profiles from different coatings, the coatings need to be of similar thickness. This is the case for all coatings in Table IV, except for entry 5, which will not be anymore considered in this discussion. Comparing the solvent-based coating (coating 9, Table II) to an aqueous one with a relatively close composition (coating 3, Table II), it is interesting to note that the release from the solvent coating is faster than from the aqueous coating (Fig. 7). At this time, we do not have any suitable explanation for this fact. Since the solvent coating is not transparent, we will focus the rest of our discussion on aqueous-based coatings. Aqueous coatings are also not transparent (due to water uptake), but this phenomenon only slowly appears after several days and is totally reversible upon drying, as seen earlier.

Release profiles are expected to mostly depend on the diffusion coefficient of SeaNine 211 in the coating. No experimental attempts have been made to measure the AF diffusion coefficient either in the core or in the shell of the coating but it is well known that diffusion coefficients of small molecules in polymeric matrixes change by several orders of magnitudes with the  $T_g$  of the polymer.<sup>26</sup> Our initial goal was to change independently the  $T_g$  of the core and of the shell; however, latexes with high shell  $T_g$  (such as 1 in Table IV) do not form continuous films upon application at room temperature. All the other latexes have shell  $T_g$  slightly below room temperature, to allow for the formation of a continuous film at room temperature (MFFT around 20°C).

For the coating with the highest core  $T_g$  (coating 2 in Table IV), release is excessively slow, whereas the release rate does not seem to significantly change when the core  $T_g$  is changed between 6.6 and 50°C



(compare coating 3, 4, 6, 7, and 8 in Table IV). In Figure 7, only the release profile of coating 4 is represented, but those of coatings 3, 6, 7, and 8 would be nearly superimposable. The film obtained from a pure PMMA latex ( $T_g$  core =  $T_g$  shell = 115°C, coating 1 in Table IV) could only be prepared at high temperature (around 90°C). The release rate from this coating is so low that it would be confounded with the  $x$  axis if reported in Figure 7. Using the empirical relationships derived by Sundberg et al. in Ref. 26, one can calculate the diffusion coefficient at 25°C of SeaNine 211 in a polymer ( $Wt_{AF} = 10\%$ ). If the  $T_g$  of the core polymer is 125°C, then the calculated diffusion coefficient of AF in the core is found to be around  $1.2 \times 10^{-15}$  cm<sup>2</sup>/s. Using this value, it is possible to estimate the time it takes for the AF to travel a distance of 120 nm and exit from the PMMA core (using  $t = l^2/D$ ). This characteristic time is of the order of 1 day. On the other hand, for a polymer with a  $T_g$  comprised between 6 and 60°C, the calculated diffusion coefficient is found to be comprised between  $10^{-7}$  and  $2 \times 10^{-12}$  cm<sup>2</sup>/s and the characteristic time to escape from a core is around a minute. Therefore, it is conceivable that the diffusion of the AF out of the core becomes rate limiting when the  $T_g$  of the core polymer is around 125°C but for lower  $T_g$ s, the core is not able to retain the AF, and the diffusion in the continuous polymeric matrix constituted by the coalescence of the shells of all latex particles is rate limiting. Thus, coatings 3, 4, 6, 7, and 8 have similar release rates because they have identical shell polymers.

The release profiles are nearly linear (zero order) with time (see Fig. 7). Importantly, release experiments have been stopped after a few months, when only a small portion of the AF has leached out. We are currently conducting longer experiments to assess whether the close to zero-order release is sustained up to near complete depletion. For a Fickian diffusion (Fick's law applied with a constant diffusion coefficient), the release profile should scale with the square root of time.<sup>27</sup> When the diffusing species acts as a plasticizer of the polymer (which is the case

**TABLE V**  
Characteristics of the Films Used in the Hexadecane Release Experiments

| Coating | $T_g$ of the core (°C) | $T_g$ of the shell (°C) | Hexadecane released after 2 months (%) | Thickness (μm) |
|---------|------------------------|-------------------------|--|----------------|
| H1      | 120                    | -24.9                   | 0.083                                  | 132            |
| H2      | 120                    | 16.2                    | 0.057                                  | 170            |
| H3      | 120                    | -6.6                    | 0.099                                  | 128            |
| H4      | 7.0                    | 14.6                    | 0.067                                  | 265            |
| H5      | 43.6                   | 17.1                    | 0.079                                  | 176            |
| H6      | 5.7                    | 15.6                    | 0.018                                  | 150            |
| H7      | 25.4                   | 15.6                    | 0.049                                  | 100            |

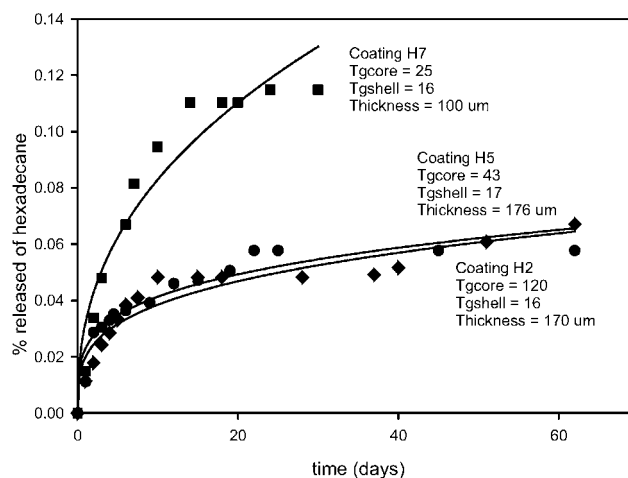


**Figure 8** Cumulative amount of released hexadecane (relative to total amount encapsulated) versus time. The lines correspond to the curve fit with  $y = ax^b$ . Squares: Experiment H7 ( $b = 0.47$ ), circles: Experiment H5 ( $b = 0.28$ ), diamonds: Experiment H2 ( $b = 0.25$ ).

here, since the  $T_g$  of the acrylic polymer is lowered by the presence of SeaNine 211), then the diffusion coefficient decreases as the diffusing species is released, resulting in release profiles which scale with time with an exponent smaller than 0.5. In our case, the release rates scale with time with characteristic exponents comprised between 0.75 and 1. In a classical approach to diffusion, the coating water interface becomes progressively depleted in SeaNine 211, resulting in an outward flux, which decreases with time (hence the square root law). In our case, it looks as if the decrease in rate caused by depletion is compensated by another phenomenon, which is currently unclear.

To try to narrow down the nature of this phenomenon, we have prepared two-stage aqueous coatings where hexadecane is nanoencapsulated (Table V). These coatings are in all regards identical to those prepared with the AF, except for the nature of the encapsulant. As in the case of SeaNine 211, the release rate depends on the nature of the coating (Fig. 8). However, in this case, the release profile scales as  $t^{0.34+/-0.12}$ . Therefore, the architecture of the coating is not responsible for the near zero-order release observed with SeaNine 211. Further work is currently in progress to try to understand this phenomenon.

## CONCLUSIONS

SeaNine 211 could be encapsulated in a straightforward fashion, by using it as a hydrophobe in a minimulsion polymerization. In this case, the SeaNine 211 is confined in nanodomains, and the resulting films formed upon drying the latex are

transparent. By contrast, phase separation occurred in a solvent-based coating. For all coatings adhesion to glass was significantly improved by applying a silanization pretreatment.

The release rate of the AF from the coating changed with the composition of the coating, but for all compositions the profile is nearly a zero-order release whereas it is nearly a Fickian type release profile when hexadecane is encapsulated. To our knowledge, there are no existing models that allow us to explain this behavior.<sup>27</sup> Based on this preliminary report, numerous questions arise. What is the rate limiting step in the diffusion process? Does the retrodiffusion of water in the coating a key component to the diffusion process? Why is the diffusion near zero-order for SeaNine 211 (at least for the first three months)? Besides assessing these questions, we are currently scrutinizing the performance of these coatings in marine conditions. Preliminary immersion in sea-water results indicate that blushing is significantly affecting the transparency of the aqueous-based coatings over time, which could prove to be a serious limitation.

We thank Professor Y. Durant for useful discussions, and the company Rohm and Haas for the generous gift of Seanine 211.

## References

1. Vicklund, R. E. *J Ind Eng Chem* 1946, 38, 774.
2. Yebra, D. M.; Kiil, S.; Johansen, K. D. *Prog Org Coat* 2004, 50, 75.
3. Youngblood, J. P.; Andruzzi, L.; Ober, C. K.; Hexemer, A.; Kramer, E. J.; Callow, J. A.; Finlay, J. A.; Callow, M. E. *Biofouling* 2003, 19(Suppl.)91.
4. Brady, R. F. *J Protective Coat Linings* 2000, 17, 42.
5. Meinema, H. A.; Rentrop, C. H. A.; Breur, H. J. A., Ferrari, J. M. *Proceedings from the First International Conference on Coatings on Glass (ICCG)*, Saarbrücken, Germany, 1997.
6. Parr, A. C. S.; Smith, M. J.; Beveridge, C. M., Cowling, M. J.; Hodgkiess, T. *Adv Mater Opt Electron* 1998, 8, 187.
7. Takahashi, K.; Ebara, M.; Mabuchi, K.; Numata, K. J. *Jpn Soc Color Mater* 2002, 75, 365.
8. Zobell, C. E. *J Mater Res* 1941, 4, 42.
9. Cortazar, M.; Egulazitbal, J. I.; Ularte, C.; Iruin, J. J. *Polym Bull* 1987, 18, 149.
10. Cheng, W. M.; Miller, G. A.; Manson, J. A.; Hertzberg, R. W.; Sperling, L. H. *J Mater Sci* 1990, 25, 1917.
11. Walheim, S.; Boeltau, M.; Mlynek, J.; Krausch, G.; Steiner, U. *Macromolecules* 1997, 30, 4995.
12. Sudol, E. D.; El-Aasser, M. S. In *Emulsion Polymerization and Emulsion Polymers*; Lovell, P. A., El-Aasser, M. S., Eds.; Wiley-VCH: Weinheim, 1997; p 699.
13. Landfester, K.; Bechthold, N.; Antonietti, M. *Macromolecules* 1999, 32, 5222.
14. Price, R. R.; Schnur, J. M. *J Coat Technol* 2003, 75, 53.
15. IUPAC-NIST Solubility Database NIST Standard Reference Database 106, [http://srdata.nist.gov/solubility/sol\\_main\\_search.asp](http://srdata.nist.gov/solubility/sol_main_search.asp).
16. Stubbs, J. M.; Sundberg, D. C. *J Coat Technol*, 2003, 75, 59.
17. Karlsson, L. E.; Karlsson, O. J.; Sundberg, D. C. *J Appl Polym Sci* 2003, 90, 905.
18. Stubbs, J. M.; Sundberg, D. C. *J Appl Polym Sci* 2004, 91, 1538.
19. Durant, Y. G.; Sundberg, D. C. *Macromolecules* 1996, 29, 8472.
20. Durant, Y. G.; Sundberg, E. J.; Sundberg, D. C. *Macromolecules* 1997, 30, 1028.
21. Brandrup, J.; Immergut, H.; Grulke, B. D. *Polymer Handbook*, 4th ed.; Wiley-VCH: Weinheim, 1999.
22. Guyot, A. *Recent Res Dev Polym Sci* 2004, 8, 207.
23. Zobell, C. E. *J Mater Res* 1941, 4, 42.
24. Vasintha, N.; Sundberg, D. C.; Rittschof, D. *Biofouling* 1995, 9, 1.
25. Miller, G. A.; Lovergrove, T. *J Coat Technol* 1980, 52, 69.
26. Karlsson, O. J.; Stubbs, J. M.; Sundberg, D. C. *Polymer* 2001, 42, 4915.
27. Neogi, P. *Diffusion in Polymers*; Marcel Dekker: New York, 1996.